Non-adiabatic molecular dynamics on graphics processing units: performance and application to rotary molecular motors

Laurens D. M. Peters,[†] Jörg Kussmann,[†] and Christian Ochsenfeld[*,†,‡]

[†]*Chair of Theoretical Chemistry, Department of Chemistry, University of Munich (LMU), Butenandtstr. 7, D-81377 München, Germany*

[‡]*Max Planck Institute for Solid State Research, Heisenbergstr. 1, D-70569 Stuttgart, Germany*

E-mail: c.ochsenfeld@fkf.mpg.de

Contents

1 Structures **2**

2 Performance **2**

3 Illustrative Examples **5**

3.1 Validation 5

3.2 Relaxed Difference Densities 8

3.3 Excited State Gradients and Non-adiabatic Coupling Vectors 10

3.4 Dihedrals 12

1 Structures

All optimized structures and initial conditions (structure and velocity) are available at `https://www.cup.uni-muenchen.de/pc/ochsenfeld/download/`.

2 Performance

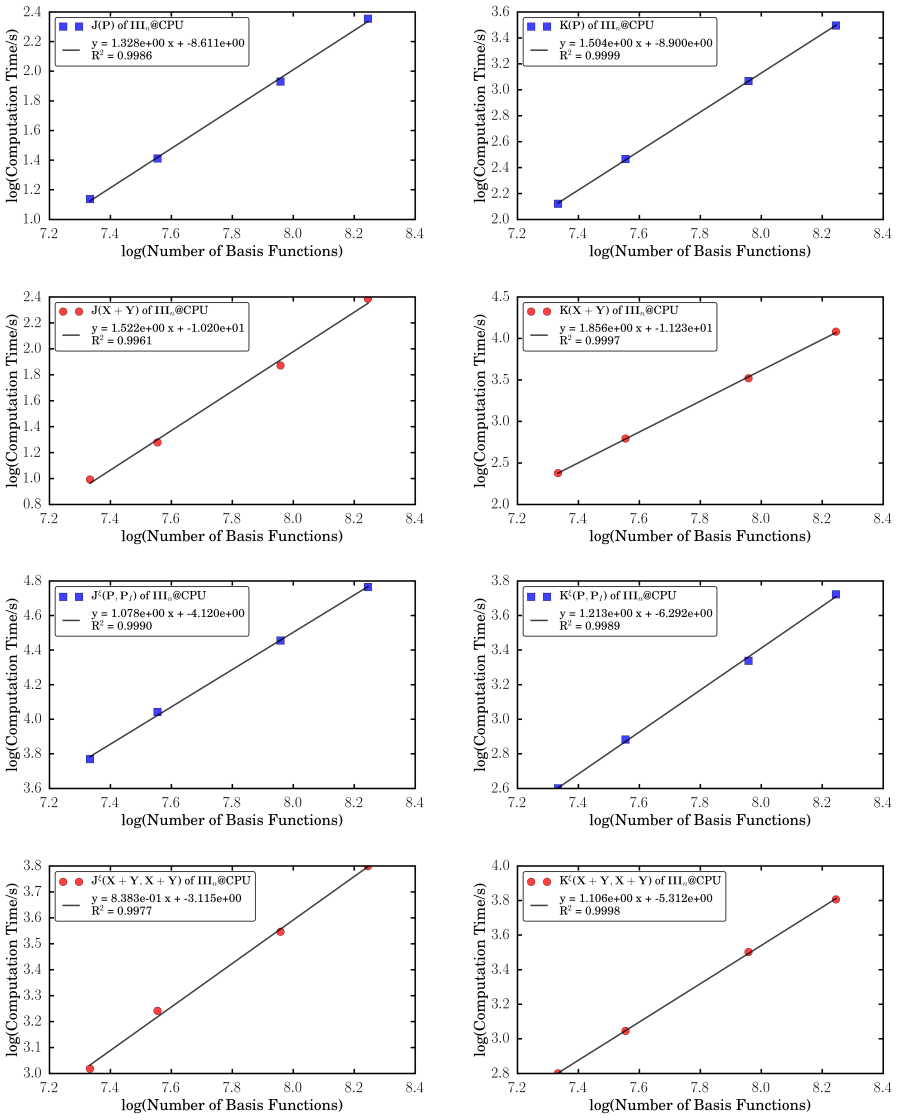

Figure S1: Log-log plot of the timings of (left) Coulomb and (right) exchange integral evaluations and their derivatives with respect to the nuclear coordinates of polyethine ($\mathbf{III}_n$) with $n = 40, 50, 75, 100$ calculated at PBE0/def2-SVP level of theory on CPUs. The slope of the linear fit is equal to the effective scaling behavior of the routine.

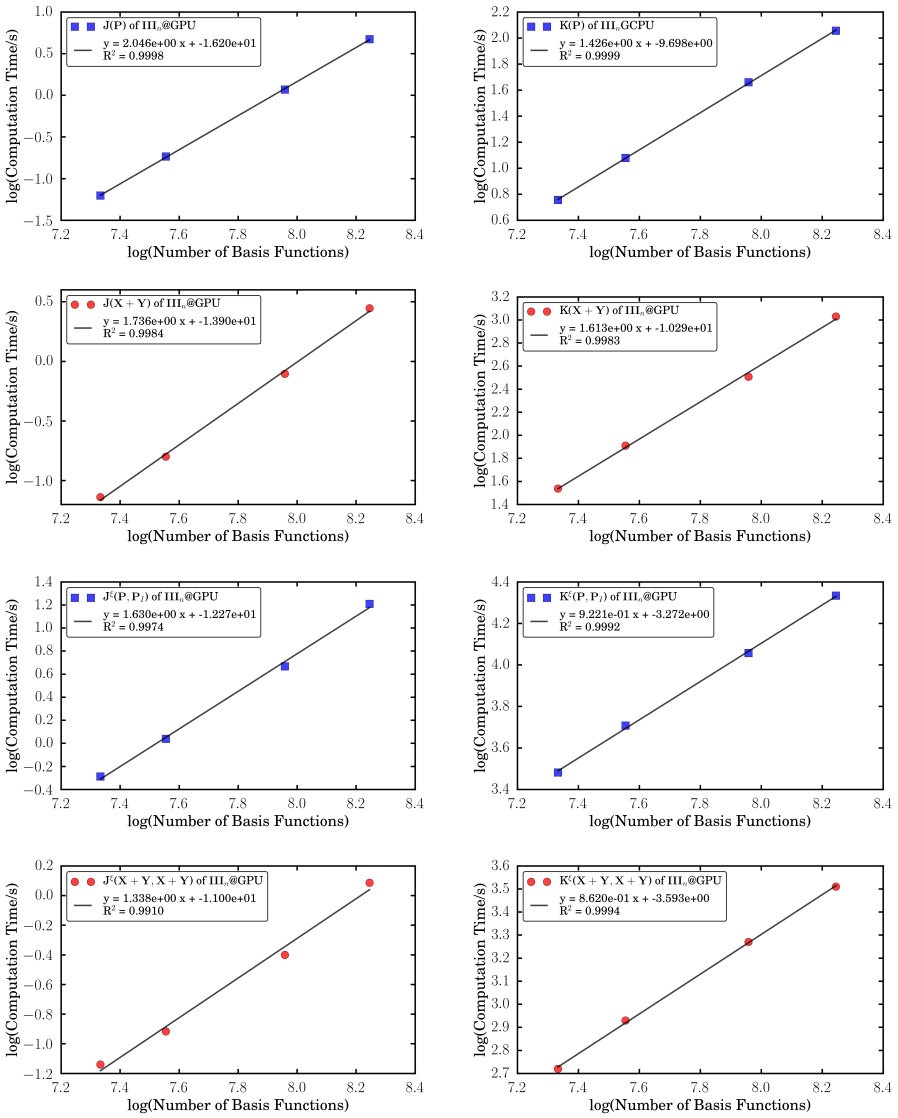

Figure S2: Log-log plot of the timings of (left) Coulomb and (right) exchange integral evaluations and their derivatives with respect to the nuclear coordinates of polyethine ($\mathbf{III}_n$) with $n = 40, 50, 75, 100$ calculated at PBE0/def2-SVP level of theory on GPUs. The slope of the linear fit is equal to the effective scaling behavior of the routine.

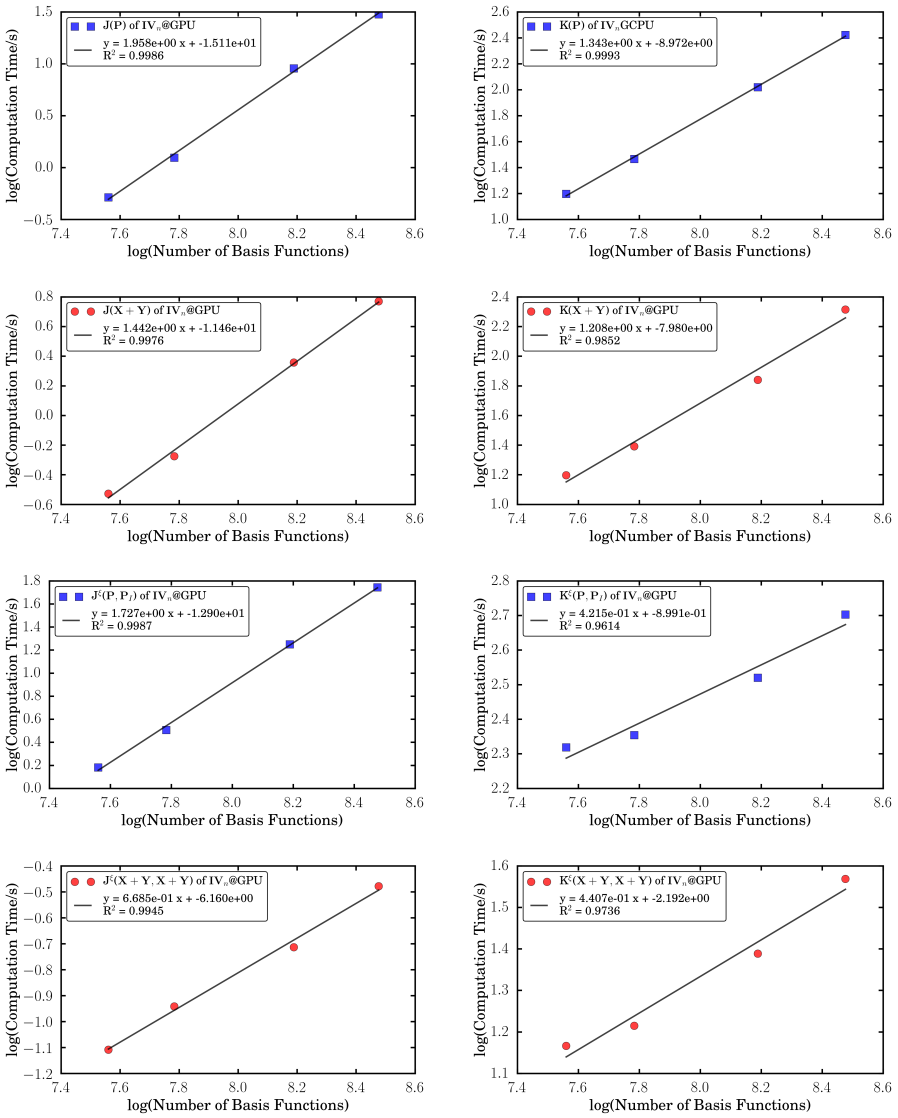

Figure S3: Log-log plot of the timings of (left) Coulomb and (right) exchange integral evaluations and their derivatives with respect to the nuclear coordinates of dialkylethene ($\mathbf{IV}_n$) with $n = 40, 50, 75, 100$ calculated at PBE0/def2-SVP level of theory on GPUs. The slope of the linear fit is equal to the effective scaling behavior of the routine.

3 Illustrative Examples

3.1 Validation

Table 1: Mean absolute errors (MAE; in atomic units) of excited state energies (ω_I), gradients (ω_I^ξ), and non-adiabatic coupling vectors ($\tau_{I\to J}^\xi$) of the four rotary molecular machines (**C**, **N**, **S**, and **O**) calculated at RPA and TDA (ωB97/def2-SVP) level of theory on GPUs, comparing two different thresholds for preLink (ϑ_{pre}), the preLink gradient ($\vartheta_{\text{pre}}^\nabla$), and the TDDFT convergence (ϑ_{TDDFT}).

Screening Thresholds and Convergence Criteria	
ϑ_{pre}	10^{-3} vs 10^{-4}
$\vartheta_{\text{pre}}^\nabla$	10^{-10} vs 10^{-11}
ϑ_{TDDFT}	10^{-5} vs 10^{-6}

C		
	RPA	TDA
MAE(ω_1)	3.19 $\times 10^{-4}$	6.55 $\times 10^{-7}$
MAE(ω_1^ξ)	4.03 $\times 10^{-5}$	4.34 $\times 10^{-6}$
MAE($\tau_{0\to 1}^\xi$)	9.89 $\times 10^{-4}$	2.71 $\times 10^{-5}$

N		
	RPA	TDA
MAE(ω_1)	1.98 $\times 10^{-4}$	2.90 $\times 10^{-6}$
MAE(ω_1^ξ)	2.42 $\times 10^{-5}$	1.22 $\times 10^{-5}$
MAE($\tau_{0\to 1}^\xi$)	9.43 $\times 10^{-4}$	6.34 $\times 10^{-5}$

S		
	RPA	TDA
MAE(ω_1)	3.91 $\times 10^{-4}$	1.09 $\times 10^{-6}$
MAE(ω_1^ξ)	2.84 $\times 10^{-5}$	8.33 $\times 10^{-6}$
MAE($\tau_{0\to 1}^\xi$)	7.85 $\times 10^{-4}$	4.32 $\times 10^{-5}$

O		
	RPA	TDA
MAE(ω_1)	1.94 $\times 10^{-4}$	9.07 $\times 10^{-7}$
MAE(ω_1^ξ)	2.82 $\times 10^{-5}$	7.30 $\times 10^{-6}$
MAE($\tau_{0\to 1}^\xi$)	6.35 $\times 10^{-4}$	3.59 $\times 10^{-5}$

Table 2: Mean absolute errors (MAE; in atomic units) of excitation energies (ω_I), gradients (ω_I^ξ), and non-adiabatic coupling vectors ($\tau_{I\to J}^\xi$) of the four rotary molecular machines (**C**, **N**, **S**, and **O**) calculated at RPA and TDA (ωB97/def2-SVP) level of theory on GPUs, comparing RPA and TDA.

RPA vs. TDA

	C	**N**	**S**	**O**
MAE(ω_1)	6.49 $\times 10^{-3}$	8.17 $\times 10^{-3}$	5.41 $\times 10^{-3}$	6.70 $\times 10^{-3}$
MAE(ω_1^ξ)	6.43 $\times 10^{-4}$	5.86 $\times 10^{-4}$	5.28 $\times 10^{-4}$	4.60 $\times 10^{-4}$
MAE($\tau_{0\to 1}^\xi$)	8.73 $\times 10^{-3}$	8.14 $\times 10^{-3}$	8.81 $\times 10^{-3}$	8.86 $\times 10^{-3}$

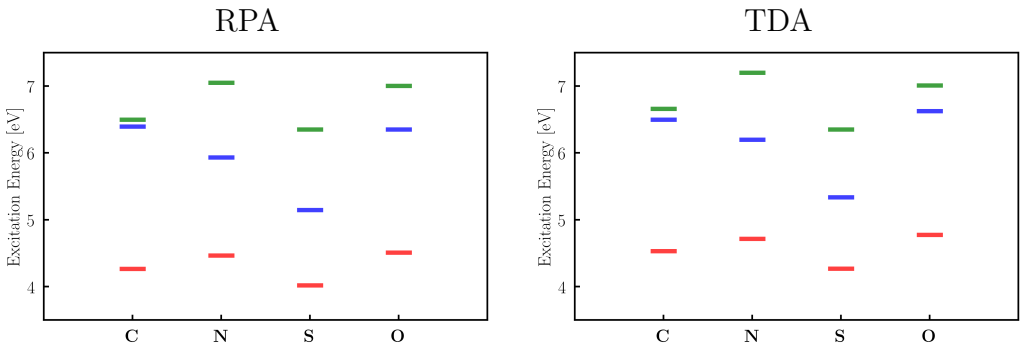

Figure S4: Excitation energies of the four rotary molecular machines (**C**, **N**, **S**, and **O**) calculated at (left) RPA and (right) TDA (ωB97/def2-SVP) level of theory.

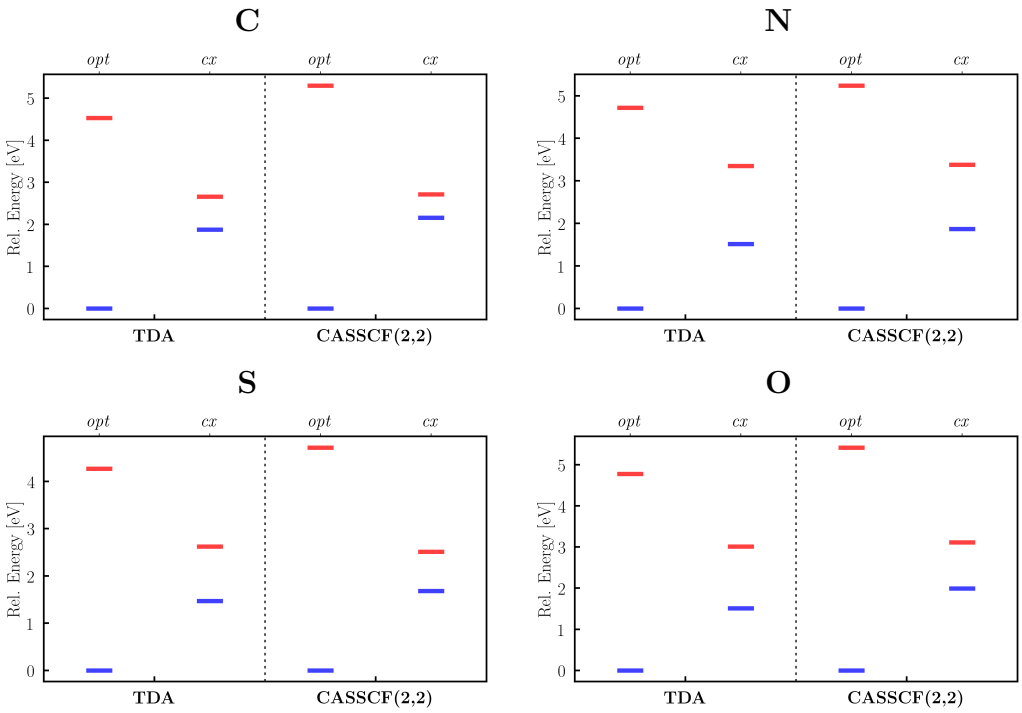

Figure S5: Comparison of relative S_0 and S_1 energies of the four rotary molecular machines (**C**, **N**, **S**, and **O**) calculated at TDA (ωB97/def2-SVP) and CASSCF(2,2)/def2-SVP level of theory. The two geometries were obtained from geometry optimizations of the ground state (*opt*) and the S_1 state (close to the conical intersection, *cx*) at TDA (ωB97/def2-SVP) level of theory. CASSCF calculations were perfomed with ORCA v4.0 (Neese, F. The ORCA program system, *Wiley Interdiscip. Rev.: Comput. Mol. Sci.* **2012**, *2*, 73-78). TDA describes both states at *cx* and trends between the different molecular machines remarkably well.

3.2 Relaxed Difference Densities

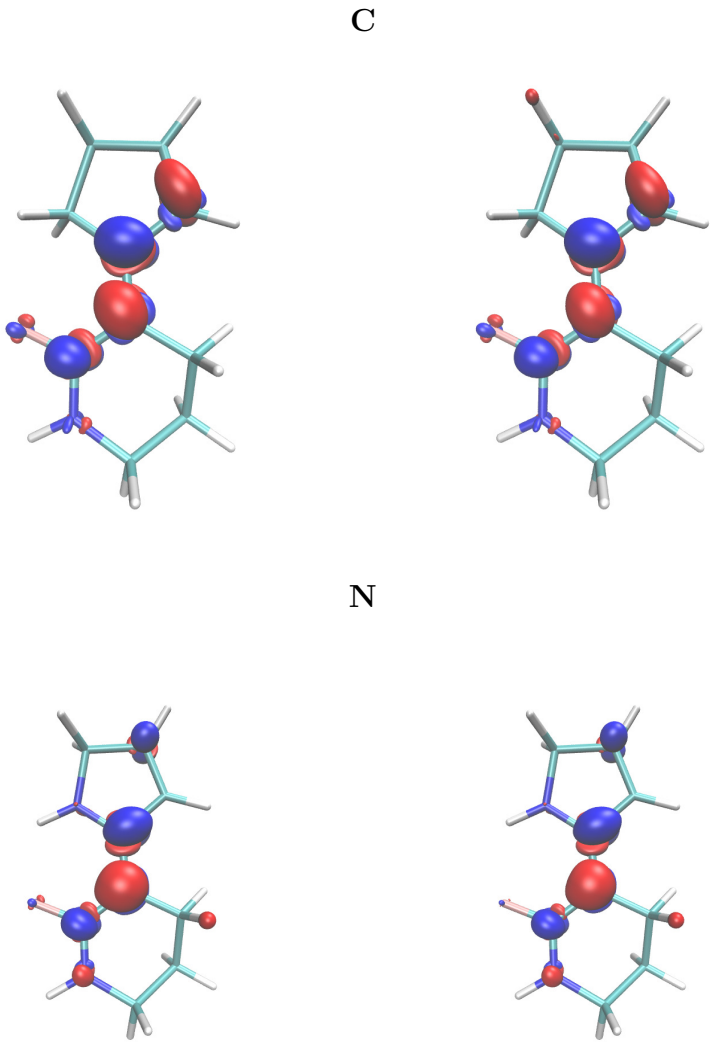

Figure S6: Plots of the relaxed difference densities of the first excited state ($\mathbf{P}_1$) of (up) **C** and (down) **N** calculated at (left) RPA and (right) TDA (ωB97/def2-SVP) level of theory.

S

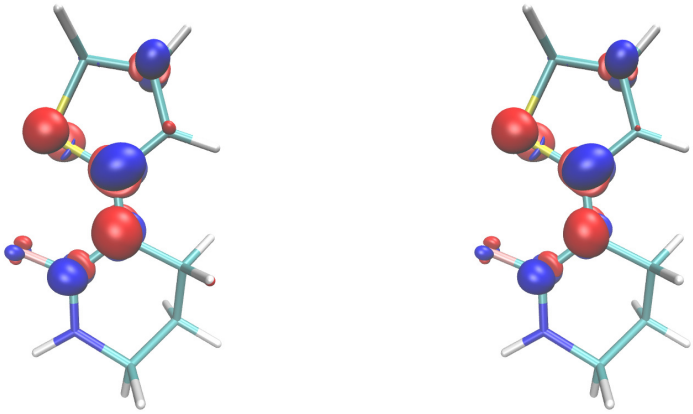

O

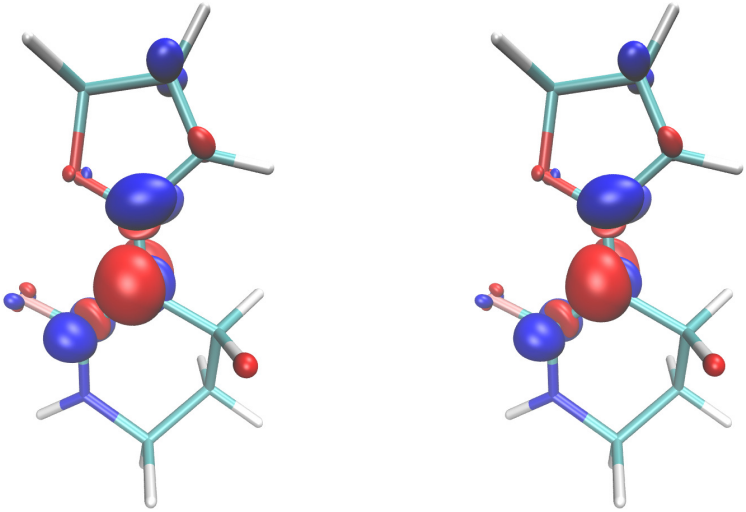

Figure S7: Plots of the relaxed difference densities of the first excited state ($\mathbf{P}_1$) of (up) **S** and (down) **O** calculated at (left) RPA and (right) TDA (ωB97/def2-SVP) level of theory.

3.3 Excited State Gradients and Non-adiabatic Coupling Vectors

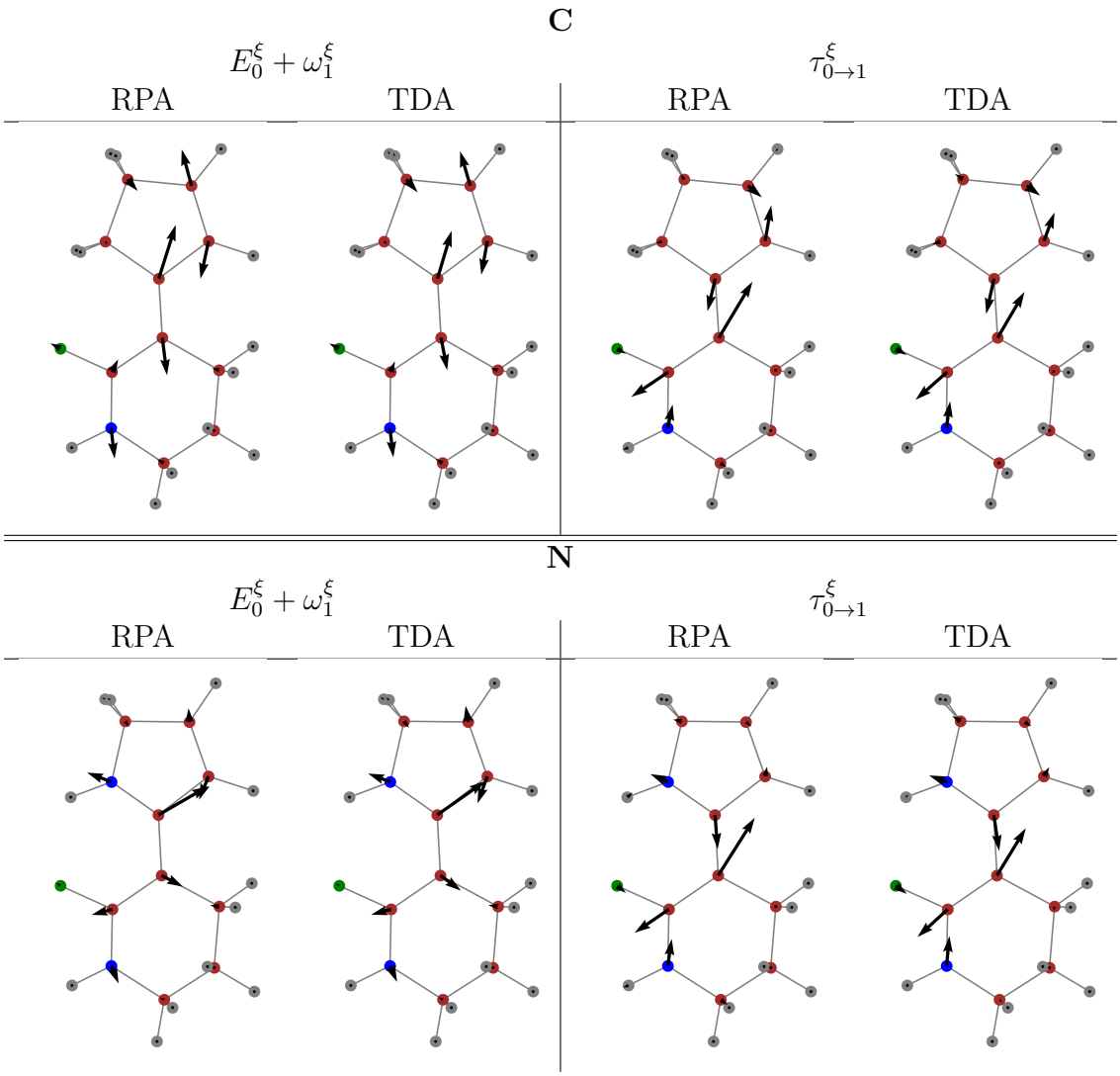

Figure S8: Excited state gradients of the first excited state ($E_0^\xi + \omega_1^\xi$) and non-adiabatic coupling vectors between the ground and the first excited state ($\tau_{0\to1}^\xi$) of (up) **C** and (down) **N** calculated at RPA and TDA (ωB97/def2-SVP) level of theory.

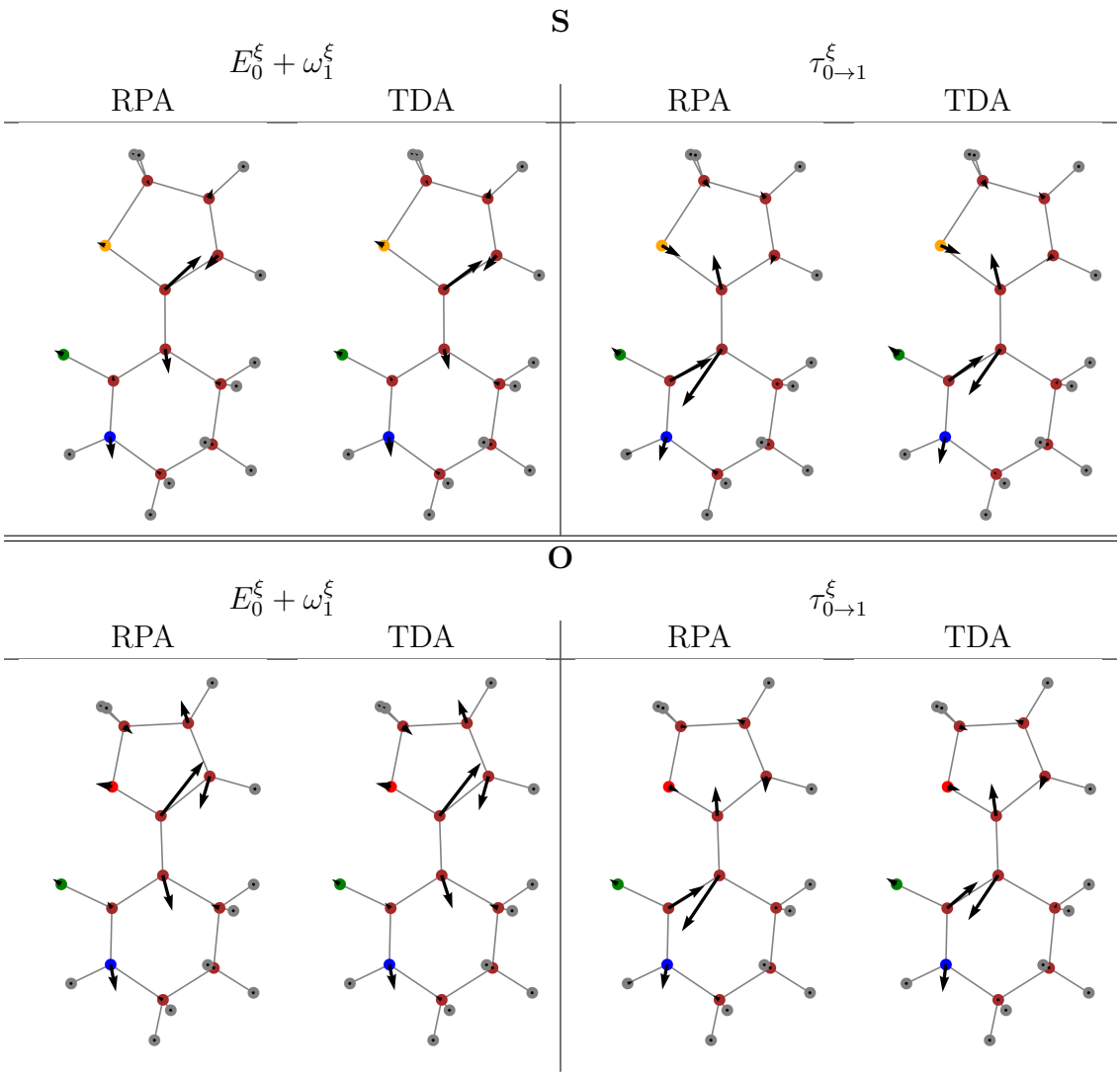

Figure S9: Excited state gradients of the first excited state ($E_0^\xi + \omega_1^\xi$) and non-adiabatic coupling vectors between the ground and the first excited state ($\tau_{0\to1}^\xi$) of (up) **S** and (down) **O** calculated at RPA and TDA (ωB97/def2-SVP) level of theory.

3.4 Dihedrals

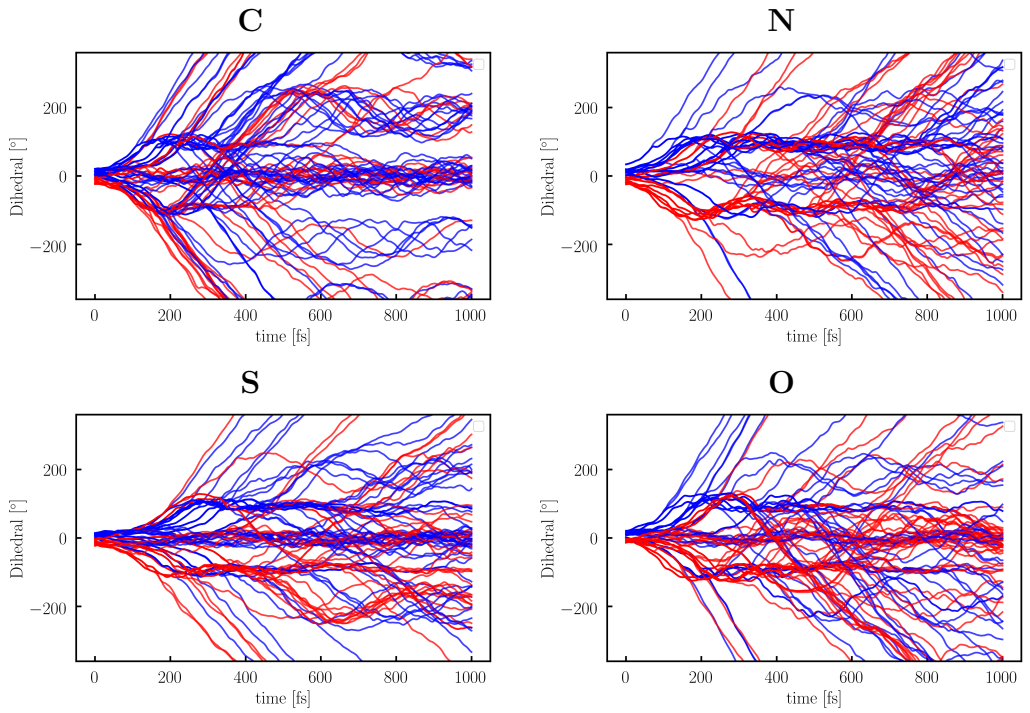

Figure S10: Dihedrals during the non-adiabatic molecular dynamics simulations of **C**, **N**, **S**, and **O**. Blue lines indicate simulations starting from a dihedral > 0 and red a dihedral < 0. All rotors show no clear preference towards clockwise (< 0) or counterclockwise (> 0) rotations.